Distribution Agreement

In presenting this thesis as a partial fulfillment of the requirements for a degree from Emory University, I hereby grant to Emory University and its agents the non-exclusive license to archive, make accessible, and display my thesis in whole or in part in all forms of media, now or hereafter now, including display on the World Wide Web. I understand that I may select some access restrictions as part of the online submission of this thesis. I retain all ownership rights to the copyright of the thesis. I also retain the right to use in future works (such as articles or books) all or part of this thesis.

Ruomin Zhu April 8, 2018

Beyond KPZ: Simulations of 1-d Surface Growth with Memory

by

Ruomin Zhu

Ilya Nemenman, Ph.D
Adviser

Department of Physics

Ilya Nemenman, Ph.D

Adviser

Stefan Boettcher, Ph.D

Committee Member

Gordon Berman, Ph.D

Committee Member

2019

Beyond KPZ: Simulations of 1-d Surface Growth with Memory

By

Ruomin Zhu

Ilya Nemenman, Ph.D

Adviser

An abstract of
a thesis submitted to the Faculty of Emory College of Arts and Sciences
of Emory University in partial fulfillment
of the requirements of the degree of
Bachelor of Sciences with Honors

Department of Physics

2019

Abstract

Beyond KPZ: Simulations of 1-d Surface Growth with Memory
By Ruomin Zhu

Growing interfaces are ubiquitous in the nature. They are categorized by different universality classes, the most well known of which is the Kardar-Parisi-Zhang (KPZ) class, which describes a variety of well-known growth processes, including sticky ballistic deposition. KPZ and other common growth processes assume that interfaces spread without memory. In contrast, recent experiments on living systems show that, in some cases, for an interface to spread, it must not slow down, and must have reached the current position only very recently. In other words, the interface possesses memory, and hence cannot be modeled by KPZ-style processes. Here we propose a model of ballistic deposition with memory aimed to describe such processes. We calculate dynamical growth exponents for this process using numerical simulations and we observe that universality classes with these exponents have not been studied before.

Beyond KPZ: Simulations of 1-d Surface Growth with Memory

By

Ruomin Zhu

Ilya Nemenman, Ph.D

Adviser

A thesis submitted to the Faculty of Emory College of Arts and Sciences
of Emory University in partial fulfillment
of the requirements of the degree of
Bachelor of Sciences with Honors

Department of Physics

2019

Acknowledgments

I would first like to thank my advisor, Dr. Nemenman. Thanks for guiding and supporting me for the past three semesters. You set an exceptional role-model as a teacher, researcher, and a father.

I would like to thank my dearest friend, Ahmed Roman. Thanks for all these enlightening talks. You expanded my skill set and got me well prepared as a researcher.

I would like to thank all members of Nemenman Lab. I learned to think about problems from different perspectives because of your brilliant, insightful ideas.

I would like to thank my parents and my girlfriend, Tiffany. Thanks for your accompany and encouragement through my hard times.

Finally, I would like to thank the department of physics. I planned to major in mathematics when I came to Emory. But the brilliance and kindness of physics people and the vibe of the whole community changed my mind. Now I am presenting my research work as a physics student.

Contents

Listing of figures

1

Background

Growing interfaces are ubiquitous in nature. Physically, the boundary of two spatial regions occupied by different substances is defined as an interface. Interfaces are formed with certain morphologies and these morphologies are mostly dynamic instead of static. The propagation of an interface through certain media is considered as growth of the interface [1]. As shown in Fig. 1.0.1, examples of growing interfaces include flux lines in a superconductor, atomic deposition, bacterial growth among many other systems.

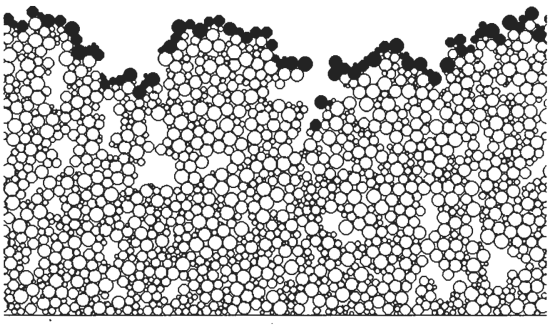

(a) Atomic deposition

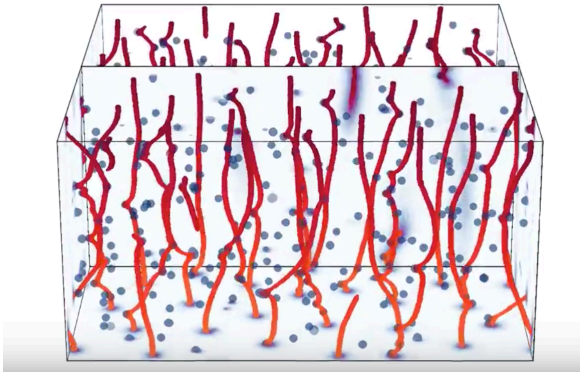

(b) Flux lines in a superconductor

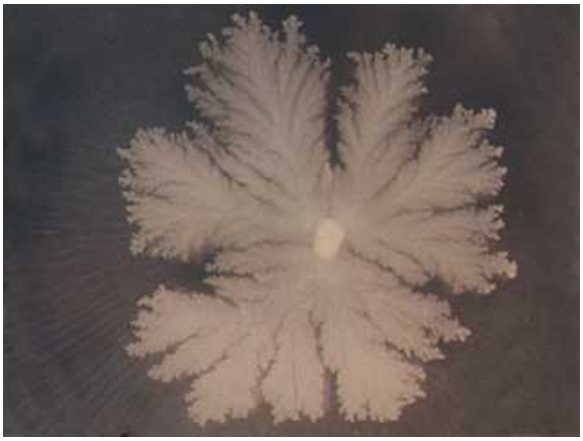

(c) Bacterial colony growth

Figure 1.0.1: Example of growing interfaces. (a) The interface generated by a simple deposition model, in which spherical particles with uniformly distributed random diameters arrive on the surface and roll until they make contact with at least two other particles (Barabasi [1]).
(b) Thermal fluctuations destroy the ordered lattice and the flux lines become wavy when temperature increases. If there are impurities in the super conductor, the flux lines are pinned in random positions of the impurities (https://www.youtube.com/watch?v=1kKMoQZ1JKo).
(c) A bacterial colony with a branched morphology (http://physionet.org/tutorials/epn/html/chp51exp3.htm).

Interfaces typically exhibit growth fluctuations, such that the width is governed by a power law. Numerous discrete and continuum models have been proposed to describe the growth profiles of interfaces, among which random deposition (RD), ballistic deposition (BD) (discrete), as well as the Edwards-Wilkinson (EW) [2] and Kardar-Parisi-Zhang (KPZ) (continuum) equations [5] are the most common ones. Growing interfaces are categorized by universality classes, which include many specific models. For example, surfaces generated by RD can be described by the EW universality class, while BD surfaces fall within the KPZ universality class.

KPZ and other common growth models come with the assumption that interfaces propagate without memory. Nevertheless, recent experiments on living systems show that, in some cases, an interface can spread at certain position only if it does not slow down and this position was reached very recently [10]. In other words, this kind of interface propagates with memory, and hence cannot be modeled by KPZ-style processes. Thus we propose a model of ballistic deposition with memory in order to describe the propagation of such interface.

This thesis is structured as follows. First, we provide a brief overview of the field of surface growth and the need for exploration of new surface growth phenomena in view of recent experiments. (Section 2). Then we present our simulations of the well-established BD class (Section 3). Finally we define a new growth process, Ballistic Deposition with Memory (BDM) and present simulations as well as analysis of the processes (section 4). We present our results of exponents in BDM as:

$$\alpha = 2.063 \pm 0.033, \qquad \beta = 1.157 \pm 0.006, \qquad z = 1.067 \pm 0.057. \tag{1.1}$$

2

Introduction

2.1 Ballistic Deposition

Surface growth is affected by many factors, yet discrete growth models can reflect the morphology and the dynamics [1] of growth while some unnecessary factors can be neglected. Various discrete growth models are used for scientific exploration, for instance random deposition, ballistic deposition, Eden model, solid-on-solid models, etc [1]. Since much of the original research in this thesis is based on modifications of the ballistic deposition model, we will devote some space

here to review this model specifically.

2.1.1 Height and Surface

Ballistic deposition (BD) was introduced by Vold [9] in 1959 as a stochastic growth model and we discuss 1-d BD in detail in this thesis. In BD, all the particles are considered equivalent square particle with size 1×1. Meanwhile, BD is defined on a lattice with length L and periodic boundary condition. The height of site x at time t is therefore $h(x, t)$. In this way, the height of surface at time t can be determined as the highest particle at each site:

$$\text{Surface height} = \{\max(h(i, t))|1 \leq i \leq L\}. \tag{2.1}$$

2.1.2 Sticking Rule

Initially, there are no particles, which means the surface is flat and $h(i, 0) = 0$ for $1 \leq i \leq L$. At each time point, one particle is dropped from far above the max height of the surface at a random position. The trajectory of the falling particle is vertical and it sticks to the first touched particle on the surface. As shown in Fig. 2.1.1, A, B, C are the falling particles while A', B', C' are their final positions deposited on the surface. Suppose at time t, one particle is dropped above a randomly picked site i, $1 \leq i \leq L$. Then the height of site i at $t + 1$ can be defined as:

$$h(i, t + 1) = \max[h(i - 1, t), h(i, t) + 1, h(i + 1, t)]. \tag{2.2}$$

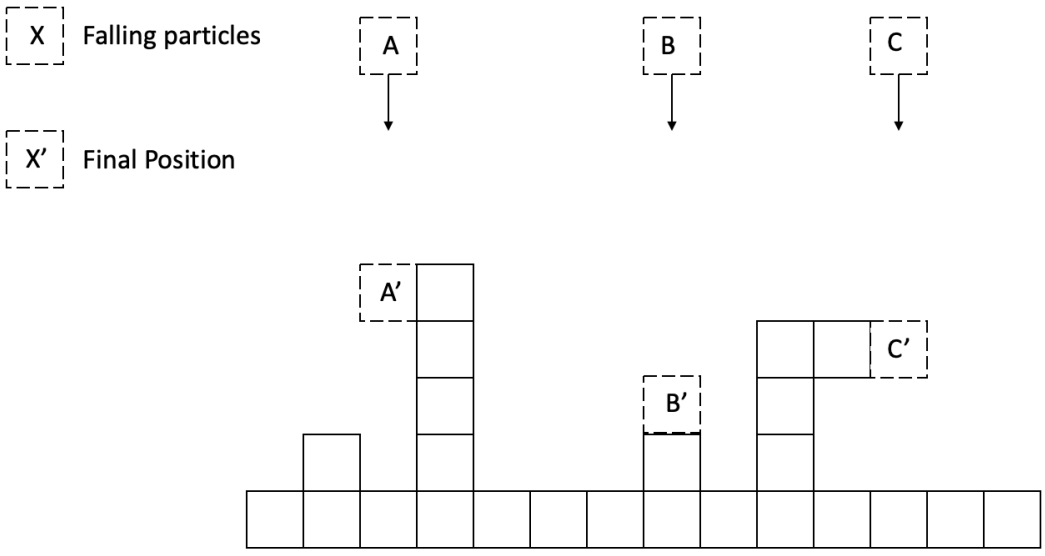

Figure 2.1.1: Mechanism of BD. Solid blocks represent the existing aggregate. Dashed blocks A, B and C are incoming particles and A', B', C' are the final positions of the particles on the surface. The final position of a particle falling on site i can be determined by $h(i, t+1) = \max[h(i-1,t), h(i,t)+1, h(i+1,t)]$.

2.1.3 Surface Roughening

As the deposition proceeds, the surface tends to have 'peaks' and 'valleys'. This is a process called *surface roughening*. With all the definitions above, some key values during roughening can be defined as follows.

Mean Height

The mean height at t, $\bar{h}(t)$, is defined as the average height of the surface:

$$\bar{h}(t) = \frac{1}{L}\sum_{i=1}^{L} h(i,t) \tag{2.3}$$

Surface Width

The width of the surface at t, which can be understood intuitively as roughness, is defined as the standard deviation of the surface height:

$$w(L,t) = \sqrt{\frac{1}{L}\sum_{i=1}^{L}[h(i,t) - \bar{h}(t)]^2}. \tag{2.4}$$

2.2 Dynamic Scaling

Dynamic scaling was introduced by Family and Vicsek [3]. It describes how width scales as a function of time and the system size in interface growth models. With fixed lattice length L, the plots of function $w(L,t)$ in log scale usually have three regimes: Poisson regime, growth regime and saturation regime as shown in Fig. 2.2.1.

Poisson Regime

When the deposition begins, the particles have to stack up for several layers until significant correlations emerge. Therefore, the initial part of the plot is a regime dominated by Poisson noise [8], where particles are deposited in an uncorrelated fashion, shown as the green segment in Fig. 2.2.1. Power law growth of this regime can be summarized as:

$$w(L,t) \sim t^{0.5}. \tag{2.5}$$

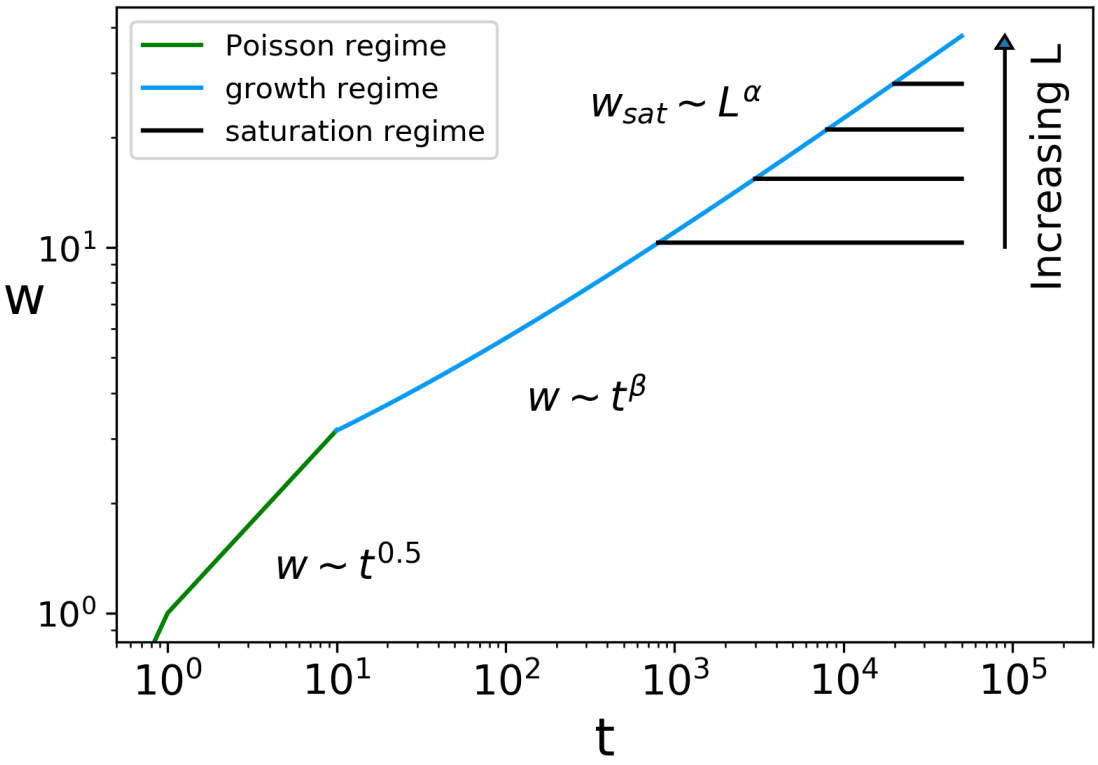

Figure 2.2.1: Expected shape of $w - t$ plots in BD. The width (w) vs time (t) graph is composed of three regimes on log-log scale: the Poisson regime (green segment), the growth regime (blue segment) and saturation regimes (black horizontal lines). Systems with larger lattice sizes (L) saturate at larger width.

Growth Regime

Indicated as the blue part in Fig. 2.2.1, the width will keep its power law increase described by:

$$w(L,t) \sim t^{\beta} \qquad t \ll t_{sat}, \tag{2.6}$$

where β denotes the growth exponent and t_{sat} represents the separation of growth regime and saturation regime.

Saturation Regime

The width will rather reach a constant value, w_{sat} after long time of deposition as fig. 2.2.1 shows. The width now will depend on the system size (L) only:

$$w_{sat}(L) \sim L^{\alpha} \qquad t \gg t_{sat}, \tag{2.7}$$

where α denotes the saturation exponent that reflects the saturated width of the surface.

The saturation time could be measured roughly by finding the intersection of the fitting lines for growth regime and saturation regime on log-log scale. It has power law relation with lattice size as well:

$$t_{sat} \sim L^{z}, \tag{2.8}$$

in which z is also know as the dynamic exponent.

Scaling Relation

Family-Vicsek scaling provides a way to relate all scaling exponents of the BD problem, as well as other growth problems [3]. Specifically, if one plots the curves with different system sizes on the same figure and the growth regimes are shown to be collapsing. Then the plots of $w(L,t)/w_{sat}(L)$ as a function of t come with the saturation regimes collapsing. Furthermore, plots of $w(L,t)/w_{sat}(L)$ as a function of t/t_{sat} for different Ls are on top of each other. This correlation indicates:

$$\frac{w(L,t)}{w_{sat}(L)} \sim f\left(\frac{t}{t_{sat}}\right). \tag{2.9}$$

By (2.7) and (2.8):

$$w(L,t) \sim L^{\alpha} f\left(\frac{t}{L^{z}}\right), \tag{2.10}$$

in which f is the scaling function satisfying:

$$f(u) \sim \begin{cases} u^{\beta} & u \ll 1, \\ 1 & u \gg 1. \end{cases} \tag{2.11}$$

For the condition $u \ll 1$ of the scaling function, $t \ll L^{z}$ has to be satisfied. Then by (2.10), (2.11), curves in the growth regime obeys:

$$w(L,t) \sim L^{\alpha-\beta z} t^{\beta}, \qquad t \ll L^{z}. \tag{2.12}$$

In the growth regime of BD, w is independent of lattice size L, which indicates:

$$\alpha - \beta z = 0, \tag{2.13}$$

finally resulting in:

$$z = \frac{\alpha}{\beta}. \tag{2.14}$$

2.3 KPZ Universality Class

2.3.1 Properties

Kardar-Parisi-Zhang equation, known as the KPZ equation, was introduced as a continuum equation to describe the profile of a growing interface [5]. KPZ equation obeys the following symmetry properties [1]:

- Invariance under translation in time.
- Translation invariance along the growth direction.
- Translation invariance in the direction perpendicular to the growth direction.
- Rotation and inversion symmetry about the growth direction.

The simplest equation satisfying the mentioned symmetries is:

$$\frac{\partial h(\vec{x},t)}{\partial t} = \nu\nabla^2 h + \frac{\lambda}{2}(\nabla h)^2 + \eta(\vec{x},t), \tag{2.15}$$

where ν deals with the surface tension, λ denotes the average velocity of the interface and $\eta(\vec{x},t)$ is the Gaussian white noise satisfying:

$$\langle \eta(\vec{x},t)\eta(\vec{x'},t')\rangle = 2D\delta^d(\vec{x}-\vec{x'})\delta(t-t'), \tag{2.16}$$

in which d denotes the dimension of the system.

2.3.2 Scaling Exponents

KPZ equation is an effective tool to explain the exponents in discrete depositions such as Ballistic Deposition. The ballistic deposition can be transformed into KPZ by limiting procedure of mathematical perturbations [6]. Width of KPZ interfaces are able to be fit into Family-Vicsek scaling (2.10). Similar to the definition in BD, the mean height and average width of multiple realizations are given by:

$$\bar{h}(t) = \frac{1}{L}\int_0^L h(x,t)dx, \tag{2.17}$$

$$w(L,t) = \sqrt{\frac{1}{L}\int_0^L [h(x,t) - \bar{h}(t)]^2}. \tag{2.18}$$

For 1-d KPZ systems, the exponents are exactly [5]:

$$\alpha = \frac{1}{2}, \qquad \beta = \frac{1}{3}, \qquad z = \frac{3}{2}. \tag{2.19}$$

Since BD falls within KPZ, the dynamic exponents of BD is the same as KPZ, and therefore given by (2.19).

3

Simulation of BD

Since the BDM model builds on the simpler BD model, we first show results of our simulations of the latter, to convince the reader that the new universality class of BDM is not due to numerical errors.

3.1 BD with different Ls

The simulation of ballistic deposition is fairly easy with the settings and sticking rules stated in Chapter 1. Since BD is a stochastic model, the characteristics are

found based on the average of multiple realizations. The mean width through all realizations is defined as:

$$w_{avg}(L,t) = \sqrt{\left\langle \frac{1}{L}\sum_{i=1}^{L}[h(i,t) - \bar{h}(t)]^2 \right\rangle}, \tag{3.1}$$

where $\langle\cdot\rangle$ takes the average over all realizations.

In order to measure the width as a function of time for different lattice sizes, time in different simulations are normalized by:

$$t = \frac{\text{Simulation Time}}{L}. \tag{3.2}$$

BD with different lattice sizes are simulated. Surface widths w as a function of time are plotted in log-log scale as Fig. 3.1.1. These curves come with the shape as Fig. 2.2.1 expected. They are apart from each other when t is small because of the Poisson noise. Then in the growth regime all curves collapse. At the end, different lattice sizes lead to different saturation times and widths as (2.7), (2.8) showed.

3.2 Scaling Exponents

As all the curves increase exponentially in growth regime, orthogonal distance regression in Scipy (Scipy.ODR) is employed to perform linear regression for $L = 2000$ data in growth regime on log-log scale and determine β as shown in Fig. 3.2.1.

Meanwhile, according to (2.7), α can be obtained by linear regression on log-log

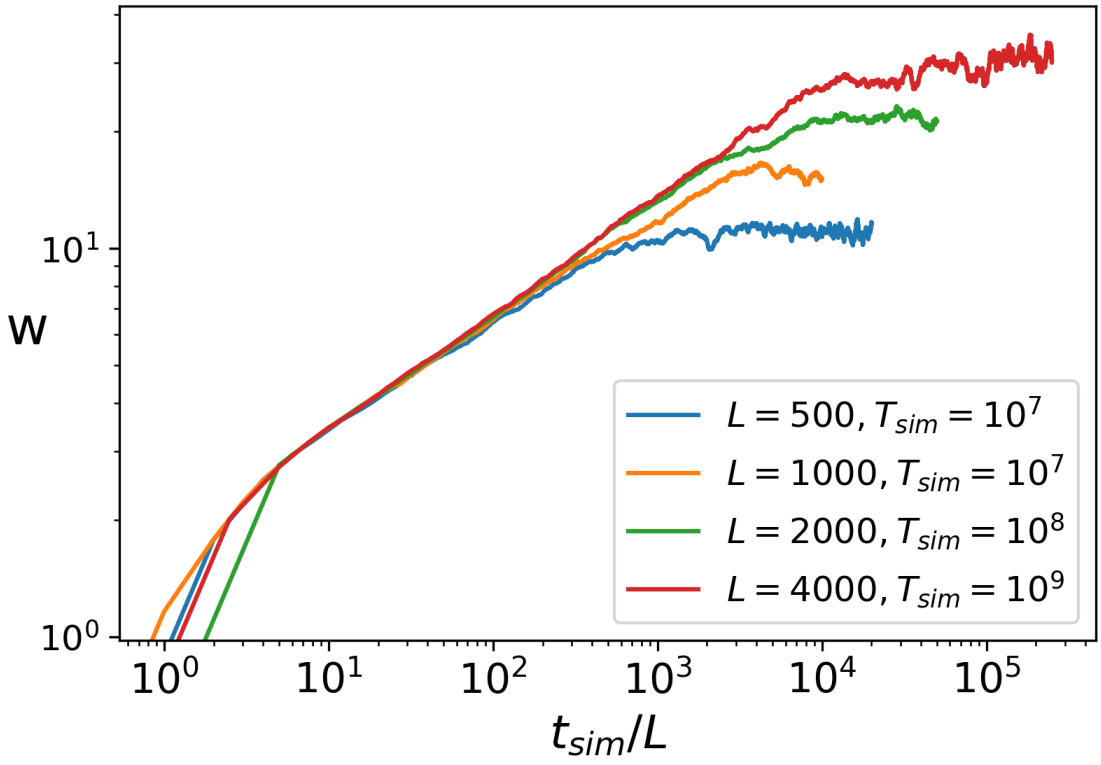

Figure 3.1.1: $w - t$ plots with different Ls in BD. Data are generated with lattice size $L = 500$, 1000, 2000, and 4000. The width is averaged over 100 realizations for each system size. Curves are plotted on log-log scale to show power law growth and saturation regimes.

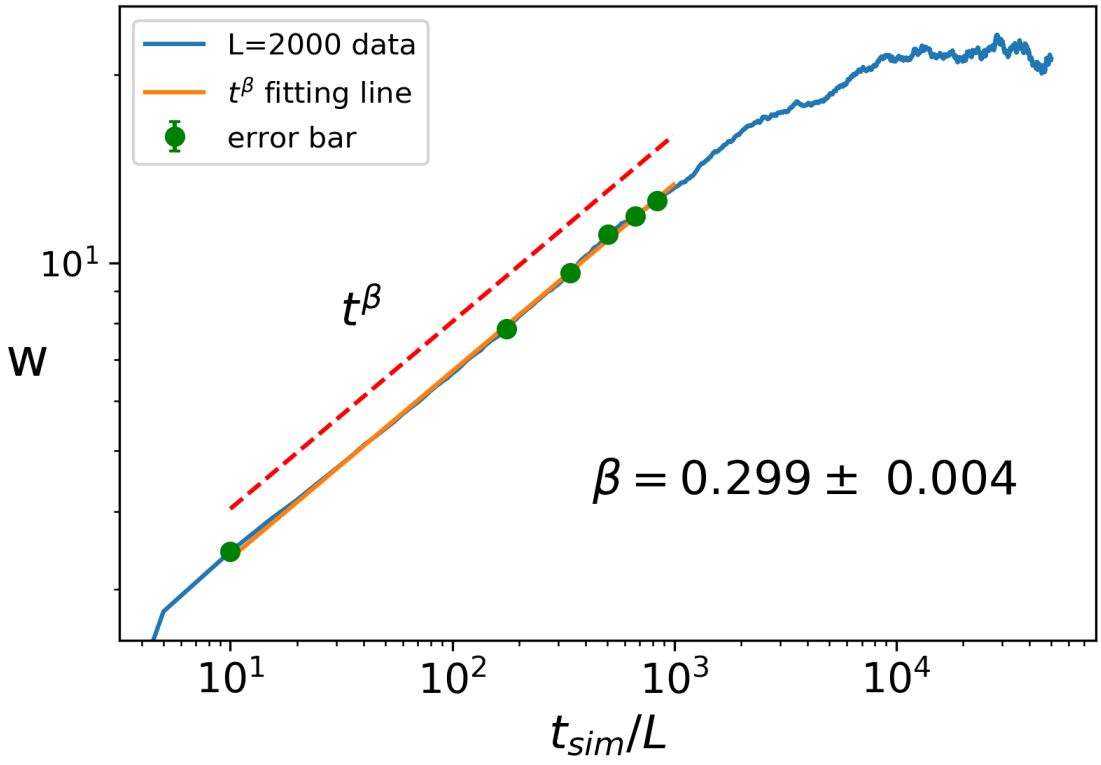

Figure 3.2.1: Linear regression for growth regime on $w - t$ plot in BD. BD simulation for $L = 2000$ shows a power law growth with $\beta = 0.299 \pm 0.004$. Two decades of simulation time $t_{sim} \in [2 \times 10^4, 2 \times 10^6]$ are used to extract the value of the growth exponent β. Only a few error bars are shown to indicate typical size of error bars.

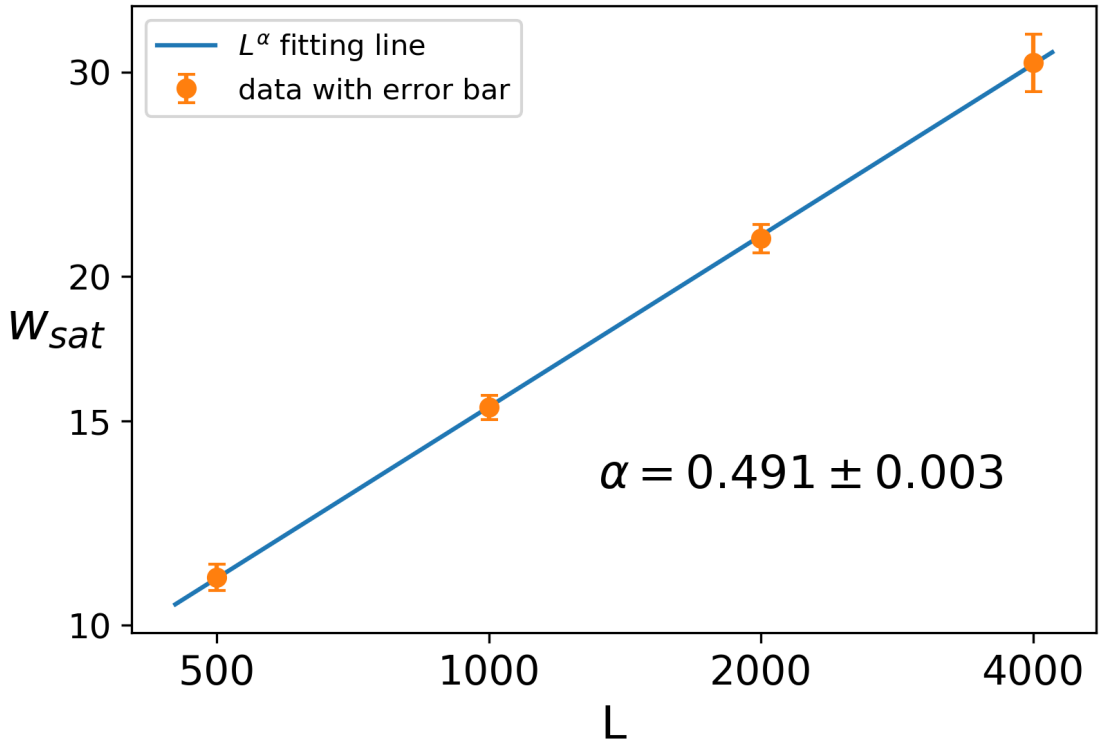

Figure 3.2.2: Linear regression for $w_{sat}(L) - L$ in BD. Values of $w_{sat}(L)$ are determined as time averages of the corresponding saturation regimes on $w - t$ curves for various system sizes (See Fig. 3.1.1). Power law relation of $w_{sat} \sim L^{\alpha}$ as expected with $\alpha = 0.491 \pm 0.003$ on log-log scale.

scale as well since:

$$\log(w_{sat}(L)) = \alpha \log(L) + C, \tag{3.3}$$

where $w_{sat}(L)$ is obtained as time average of corresponding saturation regime on $w(L,t)$ curve shown in Fig. 4.4.1. Then linear regression for $w_{sat}(L) - L$ on log-log scale is done as Fig. 3.2.2.

Thus z can be calculated:

$$\alpha = 0.491 \pm 0.003, \quad \beta = 0.299 \pm 0.004 \quad \rightarrow \quad z = \frac{\alpha}{\beta} \approx 1.64 \pm 0.03 \tag{3.4}$$

The exponents of BD are expected to be the same as KPZ. According to Reis [7] as well as Farnudi and Vvedensky [4], the exponents exhibit finite size scaling, and match the KPZ exponents only at $L \to \infty$. Family and Vicsek [3] obtained the exponents as $\beta = 0.30 \pm 0.02, \quad \alpha = 0.45 \pm 0.02$. Meanwhile, the exponents we obtained are consistent with Farnudi and Vvedensky's results of large-scale simulation with similar system size [4]. Thus BD simulation results and exponents are reliable.

4

BD with Memory

4.1 The BDM Model

Here we propose a modification of the BD model, which we believe models processes observed in biological systems, and may change the universality class of the system. The lattice and sticking rules are exactly same as BD. Yet choice of dropping site is revised. For each site on the lattice, along with the height $h(x,t)$, another profile *Propensity* $p(x,t)(0 < p \leq 1$ for all sites at any time) is introduced. The probability of deposition on a certain site depends on propensity, which has

its own dynamics, hence introducing memory into the system.

4.1.1 Dropping Rule

In BD, a particle is dropped at a site picked randomly and all sites have the same chance to be chosen. In the BDM model, the dropping site at each time step is picked by multinomial random number generated based on the distribution of propensity:

$$P_t(\text{drop at site i}) = \frac{p(i,t)}{\sum_{i=1}^{L} p(i,t)}, \tag{4.1}$$

where the propensity, $p(i,t)$ is evolved based on the memory of previous dropping history. Initially, p comes with:

$$p(i,0) = 1, \qquad 1 \leq i \leq L. \tag{4.2}$$

4.1.2 Memory Stimulation and Decay

In biological processes where activation of a cell depends on the rate of change of the messenger molecule, rather than on its value, cells can only get activated in a short period of time following the activation of their neighbors. We model this as the propensity function being stimulated by nearby activation, and then decaying with time. The mechanism of memory change is shown in Fig. 4.1.1. At time t, a particle is dropped at site j. Then for $t+1$, the propensities of site j and its adjacent neighbors will be increase to 1 while all other sites will decay exponentially by rate r $(0 < r \leq 1)$. $p(i,t+1)$ is given by:

$$p(i,t+1) = \begin{cases} 1 & j-1 \leq i \leq j+1, \\ r \cdot p(i,t) & otherwise (0 < r < 1). \end{cases} \tag{4.3}$$

The decay of propensity together with the dropping site determined by multinomial random number give us a chance to model the feature that the cell can only be activated if the temporal derivative of chemical concentration is high. Meanwhile, deposition on one site will stimulate the site itself and its nearest neighbors to 1 as well as the decay models the feature that the activation of one cell can increase the chance for itself and neighbors to be activated in a short period of time.

As one can tell from the relation, once a site is dropped on, memory of this site as well as the adjacent sites will be stimulated. The chance for these sites to be dropped on again increases. In the mean time, for other sites where there is no particle dropped on them or right next to them, their memories will decay exponentially in long term.

The simulation of ballistic deposition with memory is done with the same settings as BD. Time is normalized by the lattice size as (3.2). A snapshot of BDM surface growth is given in Fig. 4.1.2.

4.2 Effects of r

In BDM, a site can only grow in a short period of time after the growth of itself or its neighbors. As Fig. 4.2.1 indicates, value of r affects the behavior of the model drastically. For small r there is a random-walking deposition finger. The deposition is condensed around the finger while the finger itself moves around the lattice. The finger itself cannot grow much therefore only BDM growth regime appears in $w - t$ plot. When $r = 1$ the growth obeys KPZ. For intermediate r, there will be a time range where the finger itself grows with KPZ exponents, before the effects of the

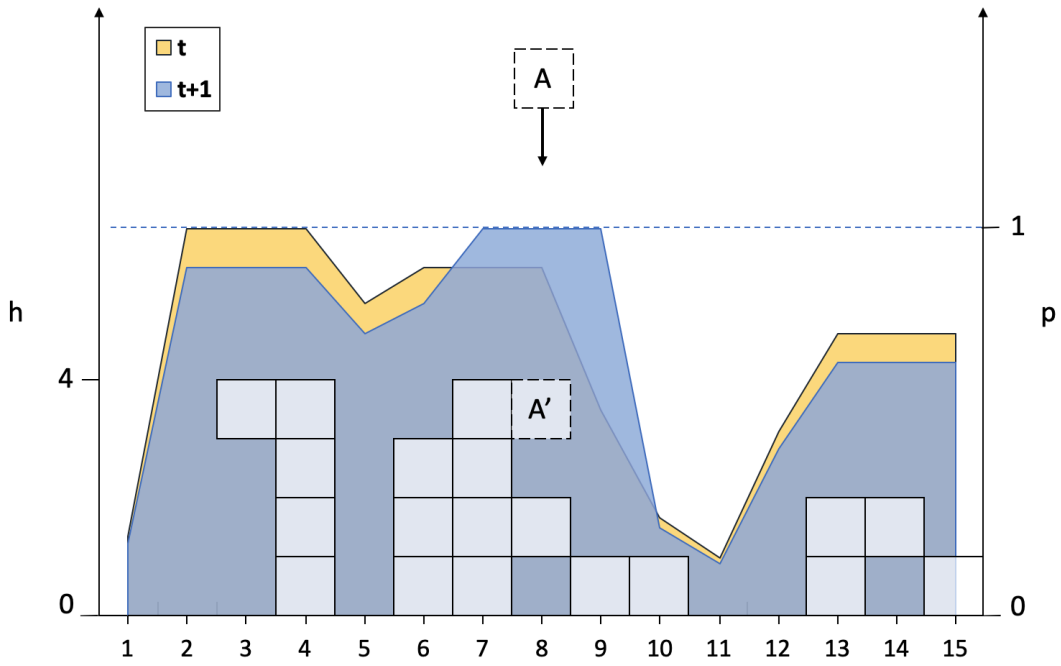

Figure 4.1.1: Mechanism of BDM. Solid blocks represent the existing aggregate. A falling particle A is deposited on the surface at site 8 (dashed block A'). The deposition of particle A stimulate the propensities of site 8 and its adjacent neighbors (site 7, 9) to 1. Propensities of other sites on the lattice decays exponentially with rate r $(0 < r < 1)$. Propensity at time t is indicated by shaded yellow area and at time $t + 1$ by shaded blue area.

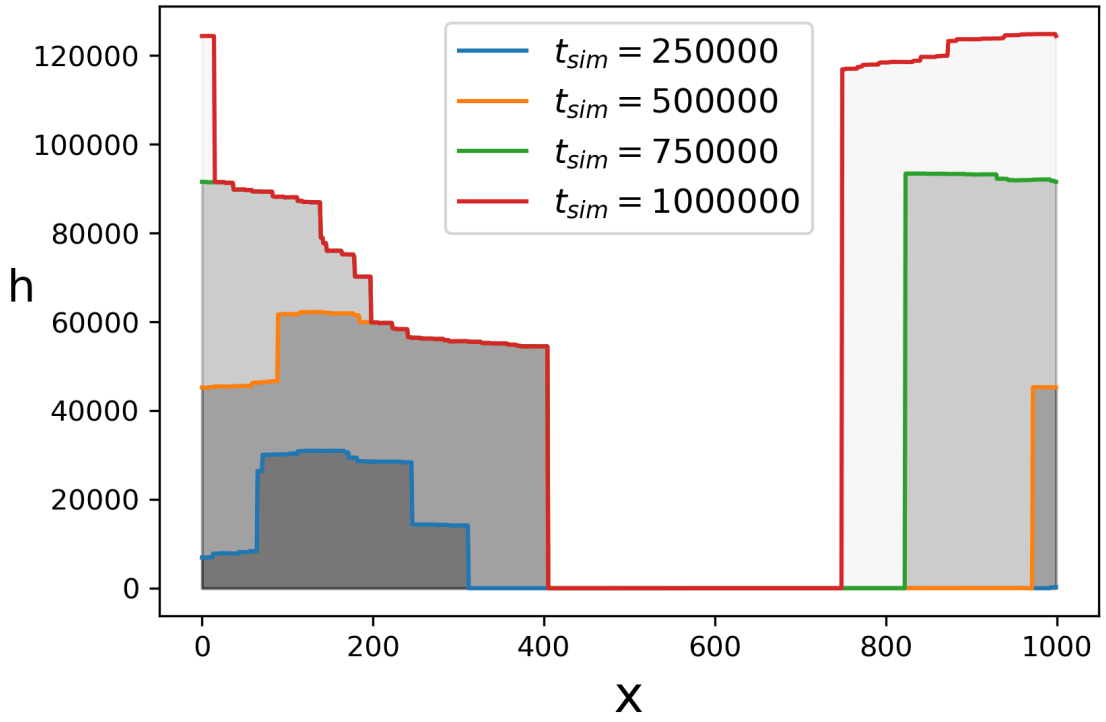

Figure 4.1.2: Snapshot of BDM growth with $r = 0.9$. The simulation is done with $L = 1000$ and $T_{sim} = 10^6$. Each line indicates a surface when t_{sim} is a multiple of 2.5×10^5. Regions with darker colors are deposited earlier.

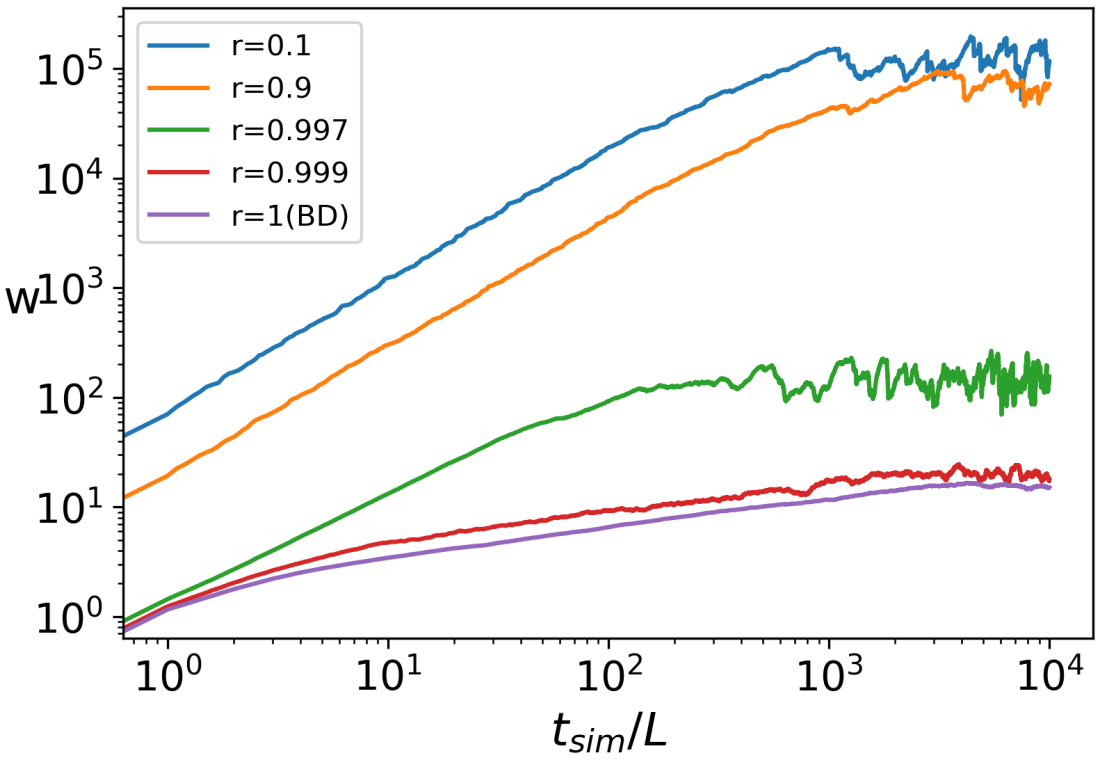

Figure 4.2.1: $w - t$ plots with different rs in BDM. All simulations are done with $L = 1000$. When $r = 1$, BDM is identical to BD. Curve for $r = 0.997$ is between two clusters of curves, hence for all remaining simulations we focus on $r \leq 0.9$ to assure that r is small enough.

finger's own motion become important. Thus, as shown in Fig. 4.2.2, there will be four growth regimes: Poisson, KPZ, the new BDM growth class and finally the saturation. For all remaining simulations, we focus on small enough values of r ($r \leq 0.9$) so that the width of the finger is only a few pixels, and the KPZ regime is absent, allowing us to focus on scaling of the new BDM growth regime.

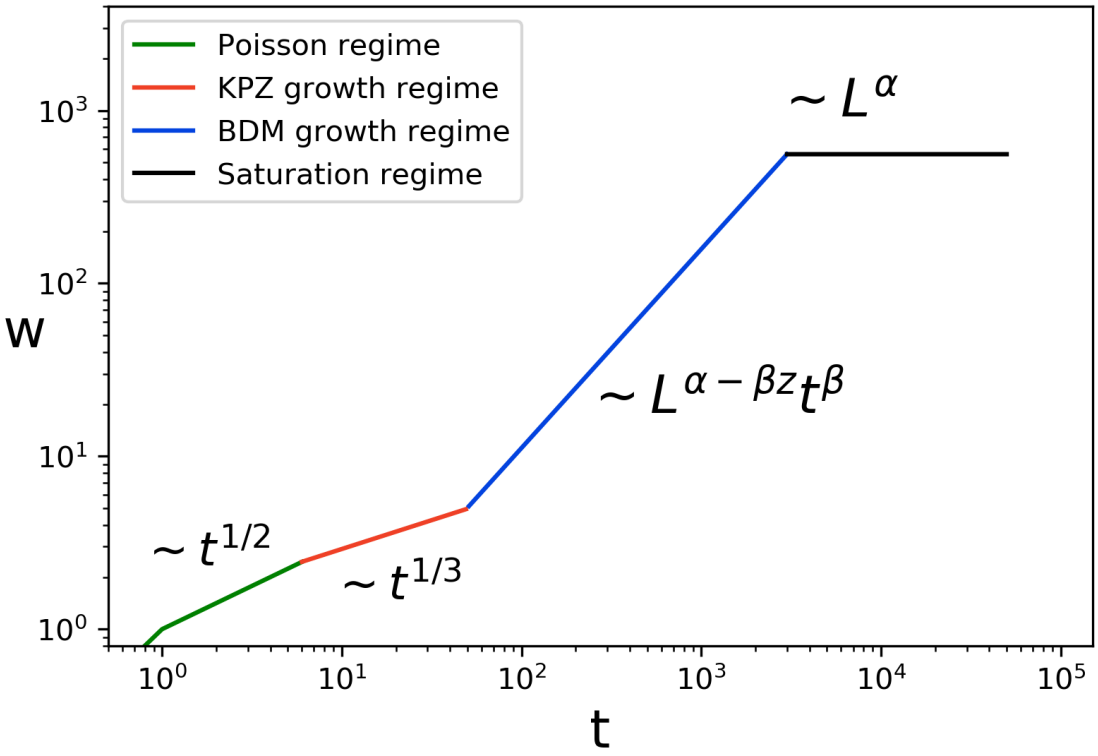

Figure 4.2.2: Expected shape of $w - t$ plots with intermediate r in BDM. The width (w) vs time (t) graph is composed of four regimes on log-log scale in BDM with intermediate r: the Poisson regime (green segment), the KPZ growth regime (red segment), the new BDM growth regime (Blue segment) and saturation regime (black horizontal lines).

4.3 Scaling Relation

In the context of BDM, Family-Vicsek scaling (2.10) holds while the scaling relation is different from BD. In BD, $\alpha - \beta z = 0$, while the BDM model will not necessarily obey this because the growth will be condensed around the deposition finger and hence roughen faster due to memory. Therefore the growth regimes of $w - t$ plots with different lattice sizes will not collapse and the expected shape of the curves are shown in Fig. 4.3.1. Here we define a new exponents γ to help describe the growth regime of BDM:

$$\gamma = \alpha - \beta z. \tag{4.4}$$

4.4 Scaling Exponents

Exponents are obtained by dynamic scaling scheme. For all the simulations in this section, $r = 0.9$ is chosen since it is effective while the growth is not extremely condensed. Surface growth as a function of time for different lattice sizes are plotted in Fig. 4.4.1.

For the saturation regime, (2.7) holds. Values of $w_{sat}(L)$ are obtained by taking average of the saturation regime on each curve. Linear regression of $w_{sat}(L)$ as a function of lattice size L in log-log scale gives the saturation exponent $\alpha = 2.063 \pm 0.033$ as shown in Fig. 4.4.2.

In the growth regime, $\alpha - \beta z = 0$ does not hold and $w - t$ curves of different lattice sizes are not on top of each other. Nevertheless, linear regression of growth

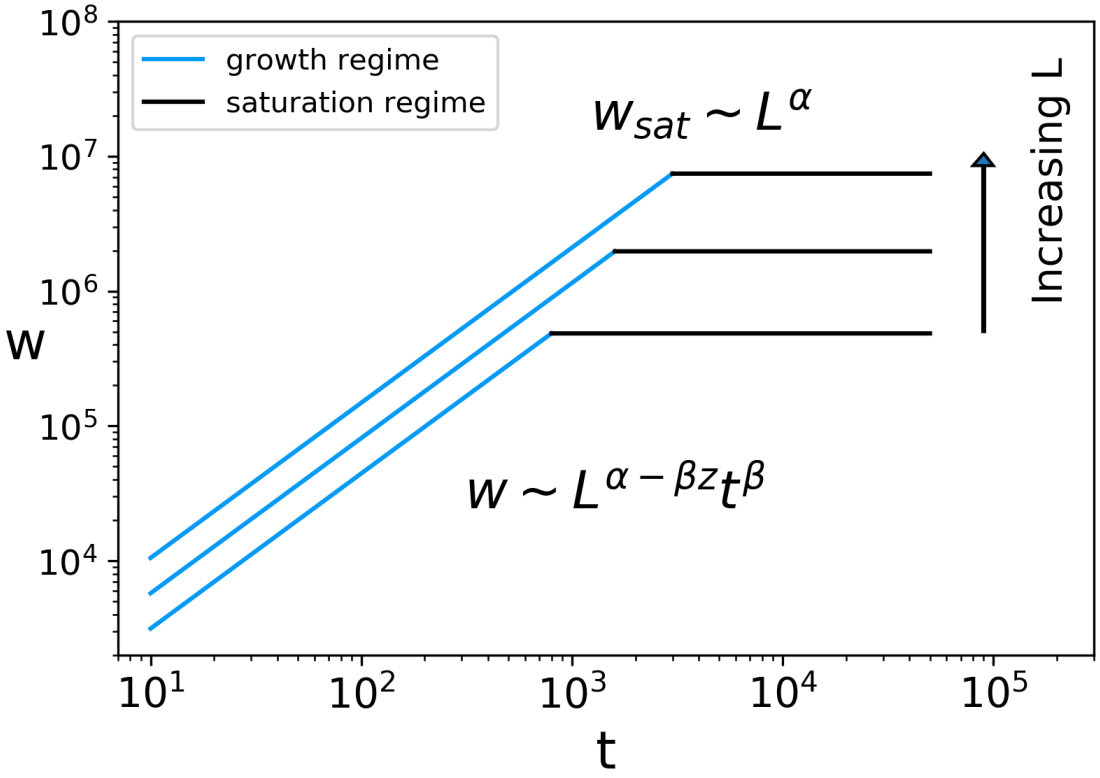

Figure 4.3.1: Expected shape of $w - t$ plots with small r in BDM. Systems with larger lattice sizes (L) have larger width (w) in all regimes. Curves do not collapse in growth regime because $\alpha - \beta z = 0$ does not necessarily hold when memory is embedded.

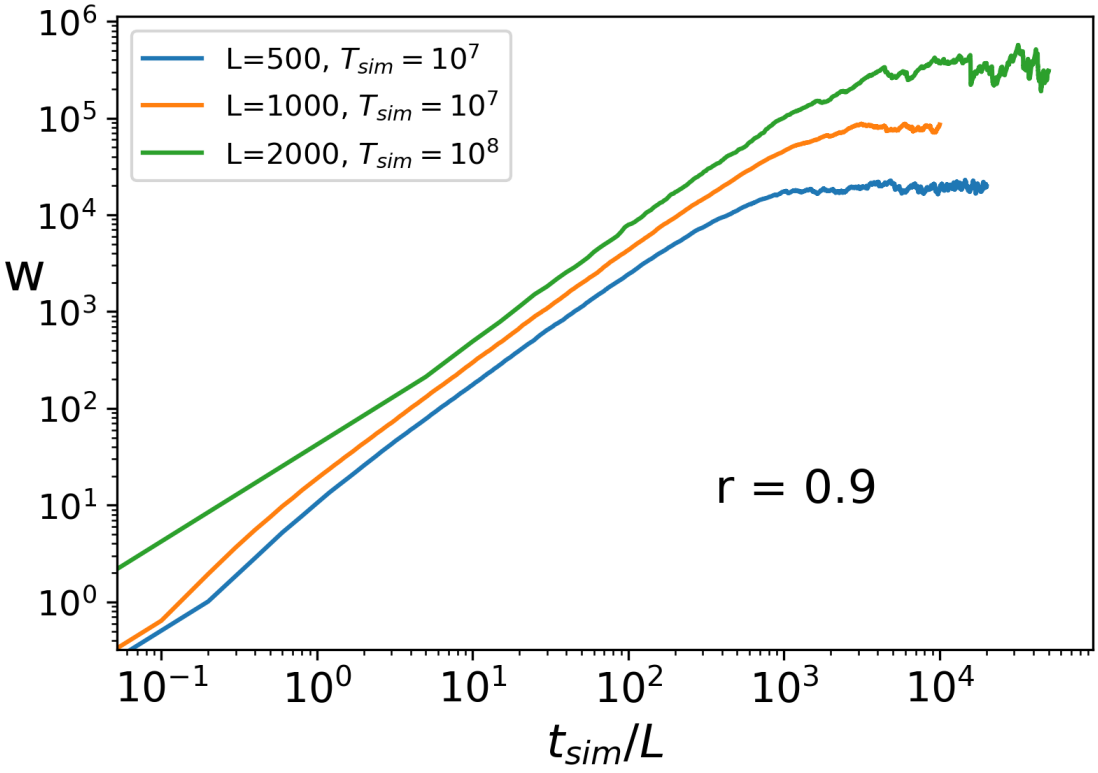

Figure 4.4.1: $w - t$ **plots with different** L**s in BDM** Data are generated with decay rate $r = 0.9$ and system sizes $L = 500, 1000, 2000$. The curves (averaged over 50 realizations) are plotted on log-log scale to show power law growth and saturation regimes. Growth regimes do not collapse because $\alpha - \beta z = 0$ does not hold in BDM.

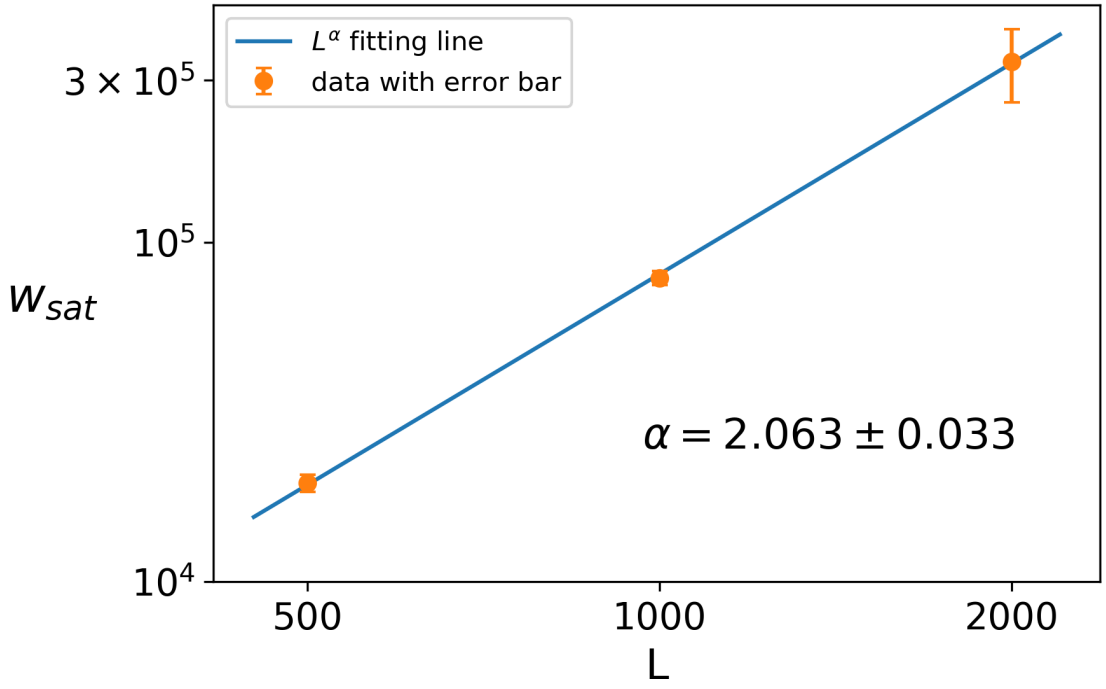

Figure 4.4.2: Linear regression for $w_{sat}(L) - L$ in BDM. Values of w_{sat} are determined as time averages of the corresponding saturation regimes on $w - t$ curves for various system sizes (see Fig. 4.4.1) with decay rate $r = 0.9$. Power law relation of $w_{sat} \sim L^\alpha$ shows as expected with $\alpha = 2.063 \pm 0.033$ on log-log scale.

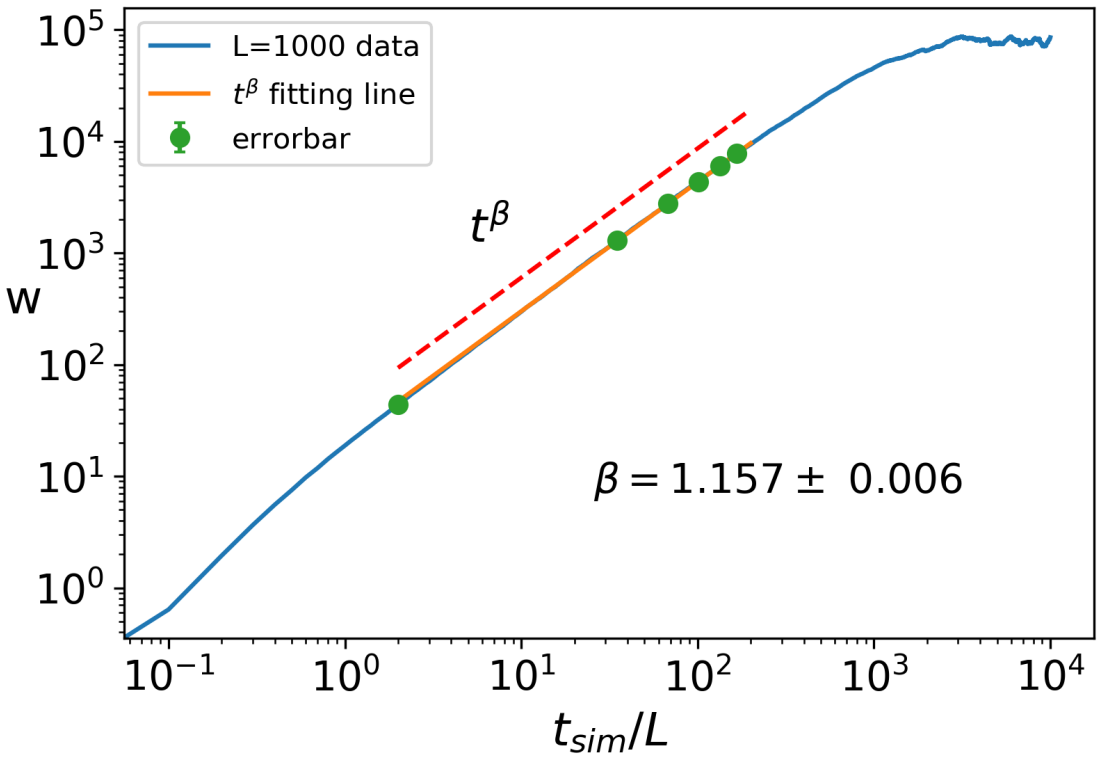

Figure 4.4.3: Linear regression for growth regime with $L = 1000$ in BDM. BDM simulation for $L = 1000$ with $r = 0.9$ shows a power law growth with $\beta = 1.157 \pm 0.006$. Two decades of simulation time $t_{sim} \in [2 \times 10^3, 2 \times 10^5]$ are used to extract the value of the growth exponent β. Only a few error bars are shown to indicate typical size of error bars.

regime in log-log scale still gives the growth exponent $\beta = 1.157 \pm 0.006$ as shown in Fig. 4.4.3 because:

$$\log(w) = C + \gamma \log(L) + \beta \log(t). \tag{4.5}$$

To determine the value of dynamic exponent z accurately, instead of finding the intersection of fitting lines, another scheme is employed. First, for the growth

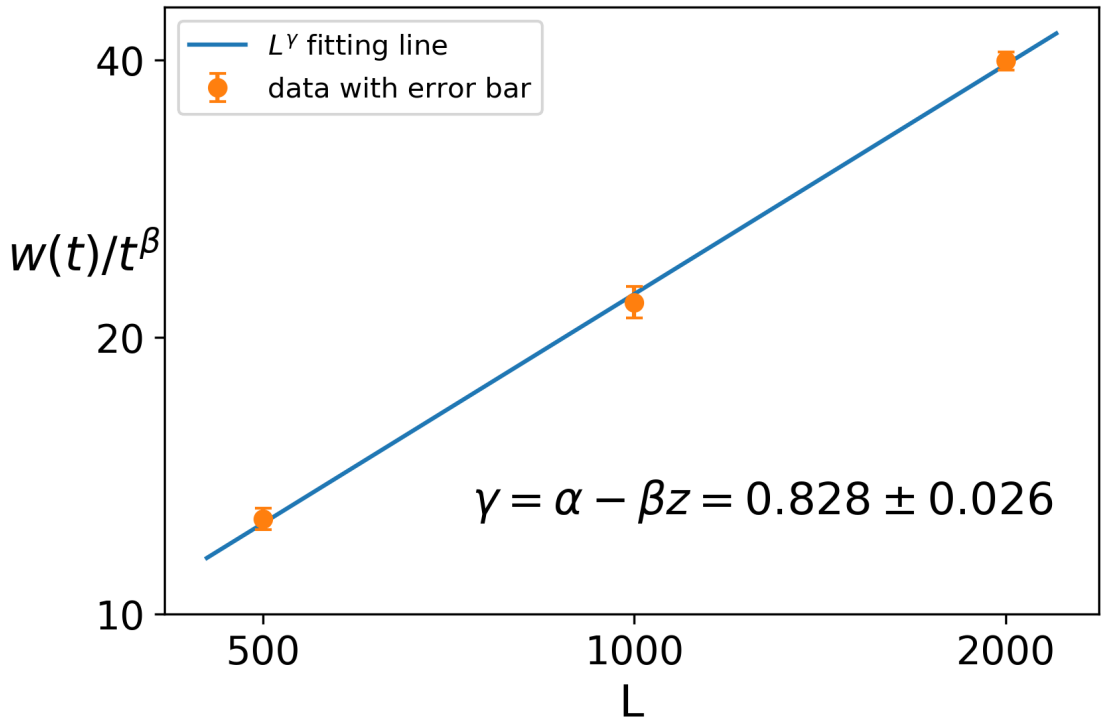

Figure 4.4.4: Linear regression for $w(L,t)/t^\beta - L$ in BDM. Values of $w(L,t)/t^\beta$ are determined as time averages of corresponding growth regimes on $w - t$ curves for various system sizes (see Fig. 4.4.1) with decay rate $r = 0.9$. Power law relation of $w(L,t)/t^\beta \sim L^\gamma$ shows as expected with $\gamma = 0.828 \pm 0.026$ on log-log scale.

regime on each curve, divide $w(t)$ by t^β governs a constant $K(L)$:

$$\frac{w(L,t)}{t^\beta} \sim L^\gamma = K(L). \tag{4.6}$$

Then, as shown in Fig. 4.4.4, linear regression for $K(L)$ vs L on log-log scale gives $\gamma = 0.828 \pm 0.026$. Together with the values of α and β obtained above, z

can be determined. We hereby present the results as:

$$\alpha = 2.063 \pm 0.033, \qquad \beta = 1.157 \pm 0.006, \qquad \gamma = 0.828 \pm 0.026,$$
$$z = \frac{\alpha - \gamma}{\beta} = 1.067 \pm 0.057. \tag{4.7}$$

The values of these exponents show a significant difference from BD exponents while the Family-Vicsek scaling still holds. Therefore one can conclude that it is a new universality class. As mentioned in chapter 3, Reis [7] suggested that dynamic exponents exhibit asymptotic relation with system size. The obtained exponents of BDM will approach their exact values as system size increases.

In this project, we verified the set up with ballistic deposition and the results showed that larger system size will lead to exponents closer to analytical results. We managed to modify ballistic deposition to include memory, hence capture the key features of growth observed by Levchenko's lab, which restricted the surface to grow only when temporal derivative of chemical concentration is high and the growing position is reached very recently. Simulation and data analysis results show that it's a new universality class. And more works will be done in the future:

- Do simulations for BD and BDM with larger system sizes.
- Verify the correlation between BD exponents and system size.
- Extrapolate the exponent from larger system sizes of BDM to find the exponent for infinite system size based on the correlation.
- Connect the exponents to experiments.
- Explore how universal the class is by slight modification on the model, like particles falling in parallel.
- Write down PDEs to describe this kind of growth.

References

[1] A.-L. Barabási and H. E. Stanley. *Fractal concepts in surface growth*. Cambridge university press, 1995.

[2] S. F. Edwards and D. Wilkinson. The surface statistics of a granular aggregate. *Proceedings of the Royal Society of London. A. Mathematical and Physical Sciences*, 381(1780):17–31, 1982.

[3] F. Family and T. Vicsek. Scaling of the active zone in the eden process on percolation networks and the ballistic deposition model. *Journal of Physics A: Mathematical and General*, 18(2):L75, 1985.

[4] B. Farnudi and D. D. Vvedensky. Large-scale simulations of ballistic deposition: The approach to asymptotic scaling. *Physical Review E*, 83(2):020103, 2011.

[5] M. Kardar, G. Parisi, and Y.-C. Zhang. Dynamic scaling of growing interfaces. *Physical Review Letters*, 56(9):889, 1986.

[6] T. Nagatani. From ballistic deposition to the kardar-parisi-zhang equation through a limiting procedure. *Physical Review E*, 58(1):700, 1998.

[7] F. A. Reis. Universality and corrections to scaling in the ballistic deposition model. *Physical Review E*, 63(5):056116, 2001.

[8] A. Schwettmann. *Ballistic deposition: global scaling and local time series.* PhD thesis, 2003.

[9] M. J. Vold. A numerical approach to the problem of sediment volume. *Journal of colloid science*, 14(2):168–174, 1959.

[10] C. J. Wang, A. Bergmann, B. Lin, K. Kim, and A. Levchenko. Diverse sensitivity thresholds in dynamic signaling responses by social amoebae. *Sci. Signal.*, 5(213):ra17–ra17, 2012.